Available online at www.sciencedirect.com
SCIENCE DIRECT®
Journal of the European Ceramic Society 25 (2005) 3157–3164
www.elsevier.com/locate/jeurceramsoc

Elimination of discolouration in reformulated bone china bodies

Ahmet Capoglu*

Department of Material Science and Engineering, Gebze Institute of Technology, P.O. Box 141, Gebze, Kocaeli, Turkey

Received 6 March 2004; received in revised form 21 June 2004; accepted 3 July 2004
Available online 16 September 2004

Abstract

In order to reduce the thermal expansion coefficient (TEC) to make it fit high scratch resistance glazes, which have lower TEC values, bone china body is reformulated. This is done by reducing the amount of bone ash, which is responsible for the formation of a crystalline phase of β-tricalcium phosphate (β-TCP) with a high TEC value and adding prefired anorthite materials, which has a lower TEC value, in the body.

Fired samples of reformulated bone china show a bluish-green tint due to iron impurities. When about 5 wt.% of ZnO was added to the reformulated bone china bodies this bluish-green tint was removed and the degree of the whiteness of reformulated body was again become similar to commercial bone chinas. The cause and elimination of discolouration of reformulated bone china have been investigated. ZnO containing reformulated bone china bodies develop zinc-spinel (gahnite, $ZnAl_2O_4$) crystals, which are the reason for the increasing whiteness of samples by incorporating iron ions into the spinel structure.

Keywords: Anorthite; Bone china; $Ca_3(PO_4)_2$; Discolouration; $ZnAl_2O_4$

1. Introduction

Bone china is a unique material in terms of its appearance, being exceptionally white and translucent makes it the world's most expensive type of tableware. Moreover, it has the greatest strength of any pottery body. However, its rather soft glaze could easily be scratched and therefore limits its use in demanding applications such as daily domestic use in restaurants and hotels.[1] Additionally, consumer concerns about the use of lead containing glazes and decoration in the ceramic tableware industry were questioned because of the toxicity of lead.[2–4] Both of these limitations on the present glaze system of bone china have forced the industry to look for new glaze systems and this has lead to the studies involving the development of leadless glazes.[5–7]

Typical composition of a modern commercial bone china is 25 wt.% clay, 25 wt.% of Cornish stone and 50 wt.% bone ash.[8,9] The microstructures of bone china are known to contain β-tricalcium phosphate (β-$Ca_3(PO_4)_2$) (β-TCP), anorthite ($CaAl_2Si_2O_8$), α-quartz (SiO_2) and calcium aluminosilicate glass.[10–14] The thermal expansion coefficient (TEC) of anorthite[15] from 20 to 500 °C is ∼4.3×10^{-6} °C^{-1}, while the TEC for glasses[12] of the compositions detected in bone china from 20 to 350 °C were calculated to be 3–4.5 × 10^{-6} °C^{-1} and the approximate TEC of β-TCP[12] from 50 to 400 °C is 12×10^{-6} °C^{-1}. The TEC of a bone china body[12] from 20 to 500 °C is known to be ∼8.4×10^{-6} °C^{-1}. Since fired bone china bodies consist of about 30 wt.% anorthite, 30 wt.% heterogeneous glass and 40 wt.% β-TCP, the value of TEC could be calculated by using simple rule of mixtures which is consistent with the relative proportions of the phases.

Designing a new glaze system having higher scratch resistance requires more silica to be present in glaze formulations. However, because of low TEC of silica[16] (0.54×10^{-6} °C^{-1}), the overall TEC value of glazes would be reduced. This would create a TEC mismatch problem with commercial bone china body.

According to simple rule of mixture, the TEC of bone china could be reduced by lowering the amount of β-TCP which in turn by lowering the amount of bone ash in body formulation. However, when the new formulations with lower

* Tel.: +90 262 6538497x1080; fax: +90 262 6538490.
E-mail address: capoglu@penta.gyte.edu.tr.

0955-2219/$ – see front matter © 2004 Elsevier Ltd. All rights reserved.
doi:10.1016/j.jeurceramsoc.2004.07.008

Table 1
Nominal compositions of a commercial and reformulated bone china bodies

Codes of composition	Bone ash	Cornish stone	Prefired material	China clay	Nepheline syenite	ZnO
Commercial bone china	50.00	25.00	–	25.00	–	–
BCM-11	35.00	–	45.00	10.00	5.00	5.00
BCM-12	35.00	–	50.00	10.00	5.00	–
BCM-13	25.00	–	55.00	12.50	7.50	–
BCM-14	25.00	–	55.00	12.50	2.50	5.00
BCM-15	25.00	–	50.00	15.00	10.00	–
BCM-16	25.00	–	50.00	15.00	5.00	5.00

bone ash content were prepared it was observed that fired samples of reformulated bone china had shown a bluish-green tint. This has been always a problem whenever the bone ash content of bone china formulation was attempted to be reduced.[17] Whiteness of bone china is one of its crucial qualities. A creamy white is the colour regarded as ideal.[8]

Yates and Ellam[18] made a study on the colour of bodies prepared with different proportions of bone ash, china clay and Cornish stone. They found that there were distinct fields of brown, green and bluish shades, but the colour could not be explained in terms of composition. Mellor[19] stated that the iron oxide impurity in bone china behaves in a very strange way because it forms iron phosphates. He found bluish crystals covered with a red crust in thin sections. Moore[20] considered that the main cause of the unwanted colouration seemed to be an improper balance between the alumina and the alkali content of the body. He found that by decreasing the clay and increasing the flux, which was Cornish stone, the green colouration decreased. Wilson[21] stated that discolouration could be caused by wrong firing atmospheres, and it is generally held that a bluish colour results when the kiln atmosphere is reducing.

Similar discolouration problem was also observed in glass manufacturing.[22] In order to eliminate unwanted colouration in glass manufacturing chemical decolourizing agents are being used. The wide range of materials used for chemical decolourising is given by Herring et al.[23] One of the materials used for chemical decolourising in glass manufacturing is ZnO. In order to see whether ZnO would have similar beneficial effect on decolourising the reformulated bone china bodies, it was decided to introduce some ZnO in body formulations of reformulated bone china. Preliminary experimental results had shown that the reformulated bone china bodies containing ZnO did not show any bluish-green tint. It was then decided to deepen the study towards understanding the effect of ZnO addition on the elimination of discolouration of reformulated bone china bodies.

In the present study the cause and elimination of discolouration of reformulated bone china have been investigated using X-ray diffraction (XRD), scanning electron microscopy (SEM), energy dispersive spectroscopy (EDS) and colorimeter techniques.

2. Experimental procedure

2.1. Body preparation and characterisation

Bone china is produced traditionally from the raw materials of bone ash, china clay and Cornish stone. For the reformulated bone china bodies, Cornish stone was replaced by nepheline syenite and prefired materials. Nominal compositions of a commercial and reformulated bone china bodies are given in Table 1. The reformulated bone china bodies were prepared with lower bone ash content than usual. The prepared compositions can be grouped into three pairs in which one composition was prepared with ZnO and the other without ZnO addition. While in one pair (BCM-11 and BCM-12) ZnO was replacing some of the prefired materials, in the other two pairs ZnO replaced some of the nepheline syenite used in body formulations. The starting materials used in body preparation had the compositions or impurity contents shown in Tables 2 and 3. The bone ash used throughout this work was kindly supplied by Josiah Wedgwood & Sons Ltd. A chemical analysis was not available but the bone ash had been finely ground with a median particle size of ∼2.5 μm. Super Standard Porcelain china clay was kindly supplied by E.C.C. International Limited (UK). The nepheline syenite was purchased from Bayer (UK) Ltd. It was the “North Cape” variety and in the as received condition had a median particle size of approximately 10 μm. In order to reduce the particle size, the nepheline syenite was wet milled. After milling, the median size of nepheline syenite particles was about 2.5 μm. High purity zinc oxide was purchased in the form of fine powders

Table 2
Chemical composition of raw materials

Raw materials used	Constituent (wt.%)								
	SiO_2	Al_2O_3	Fe_2O_3	TiO_2	CaO	MgO	K_2O	Na_2O	L.O.I.
SSP china clay	47.0	38.0	0.39	0.03	0.1	0.22	0.8	0.15	13
Nepheline syenite	56.5	23.7	0.1	0.0	1.0	0.0	8.5	7.6	1.0

Table 3
Chemical composition of zinc oxide

Constituent (wt.%)	ZnO
Assay	Minimum 99
Insoluble in H_2SO_4	Maximum 0.01
Nitrate (NO_3)	Maximum 0.003
Lead (Pb)	Maximum 0.005
Sulphur compounds (as SO_4)	Maximum 0.01
Trace impurities (in ppm)	
Arsenic (As)	Maximum 1
Chloride (Cl)	Maximum 5
Iron (Fe)	Maximum 5
Manganese (Mn)	Maximum 5

from J.T. Baker B.V. (Holland). As can be seen from Table 1 reformulated bone china bodies were prepared by using a significant proportion of a prefired material which was initially designed to be used as a starting material for novel whitewares and was developed by Capoglu and Messer.[24] The prefired material has been designed to be composed of two phases namely anorthite ($CaAl_2Si_2O_8$), as the major phase and glass as minor phase. Fig. 1 is the X-ray trace obtained from prefired material and indicates the formation of anorthite crystals, which is one of the main phases developed in modern bone china bodies. The prefired material was prepared by using mixtures of $CaCO_3$, $Al(OH)_3$, quartz, and $MgCO_3$ powders of high purity. The preparation of prefired materials was explained in detail elsewhere.[24]

For the preparation of reformulated bone china bodies all the components were wet mixed/milled for 3 h and then dried in an oven for an overnight. The completely dried powder was ground into fine powder in a porcelain mortar with a porcelain pestle. The powder was then granulated. To do this it was moistened by spraying with a fine mist of water droplets. The moist powder was then agitated and stirred with a plastic spatula to form small agglomerates. The agglomerates passing through a sieve of aperture 450 μm and retained on one with an aperture of 250 μm were collected and stored ready for use in closed plastic bottles to prevent moisture loss. Oversize and undersize agglomerates were reprocessed.

Agglomerated powders were poured into disc-shaped dies to produce test-pieces for sintering. For compaction, a die was placed between the flat platens on a hydraulic press (Moore press, 15 t capacity) and a pressure of 30 MPa was applied. The compacted test specimens were dried in the open air for 24 h. Following that the specimens were fired in a chamber furnace, heated with SiC elements (*Lenton Thermal Design UK limited*). The furnace was heated to the peak temperature at the rate of 3 °C/min and on completion of the soaking period, power to the furnace was automatically shut off and cooling rate was then dictated by the cooling rate of the furnace. The specimens generally remained overnight in the furnace before they were removed.

For XRD, powdered form of sintered samples of reformulated and commercial bone china bodies were scanned from 2θ; 5 to 70°, at a scanning rate of 1°/min, using a RIGAKU DMAX 2200 diffractometer (with Cu Kα radiation, λ = 0.154 nm) at 40 kV and 40 mA. The diffractometer was calibrated with silicon standard before use. The JCPDS cards listed in Figs. 1, 2 and 4 were used to identify crystalline phases.

For SEM observations, specimens were polished using 6, 3, and 1 μm diamond pastes after grinding with silicon carbide powders as abrasive and lubricated with water. The polished surfaces were chemically etched in 5% HF solution for 1.5 min. A Phillips XL30 ESEM TMP scanning electron microscope equipped with a tungsten electron source (operating at 15 kV) was used for microstructural examination of samples with backscattered electron images (BSE) used predominantly. Microanalysis was performed using the embedded EDX digital controller and control software.

The thermal expansion coefficients of reformulated and commercial bone china were measured using an in-house constructed dilatometer. Dense cylindrical rods were made using the technique of Jarcho et al.[25]

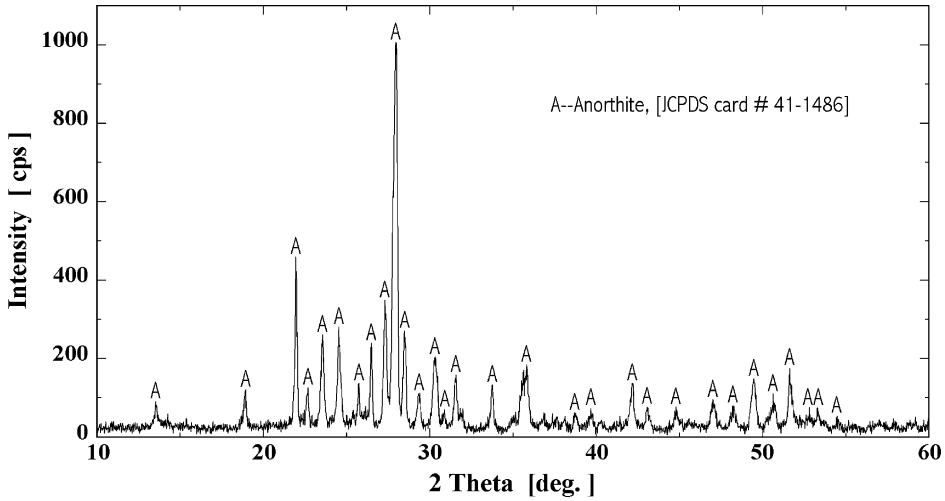

Fig. 1. XRD trace of prefired material showing anorthite formation.

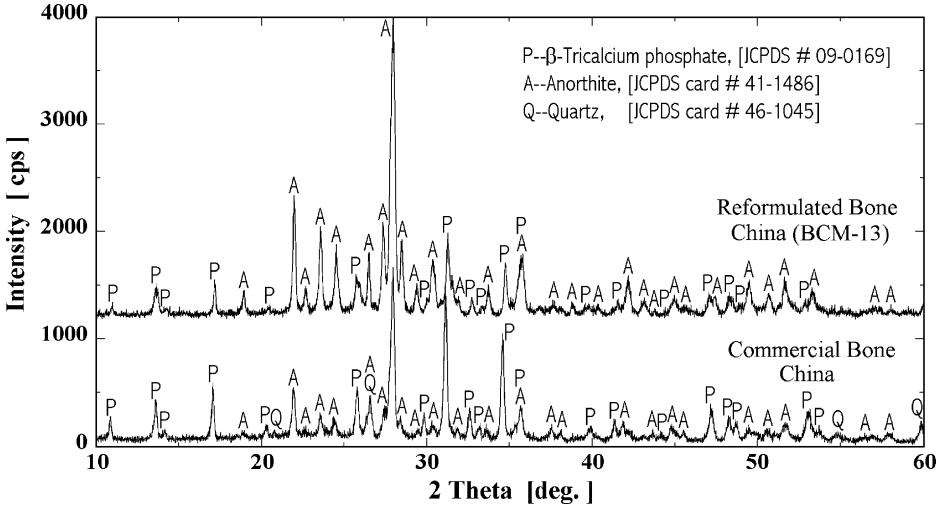

Fig. 2. XRD traces of commercial and reformulated bone china bodies.

2.2. Colour measurement

Light is visible electromagnetic radiation and white light has radiation at all wavelengths from violet at ≈400 nm to red at ≈700 nm. The colour exhibited on reflection of light by an object as perceived by an observer depends on the spectral power distribution of the illuminating source, the spectral reflectance of the object and the spectral response of the observer's eye. In order to standardise colour measurement, standards are required for both the observer and illuminate. The Commission International de l'Eclairage (CIE) in 1931 established both standard illuminates and standardised observer response curves for three primary colours, a red, a green and a blue.[26]

In the present study, the colour was measured by using a spectrometer. The spectrometer (Lambda 2, Perkin Elmer Co.) was used in the reflection mode. It operates on the CLAB colour space system in which the colour descriptors are L^*, a^*, and b^*. The $L^*a^*b^*$ system is one of many colour systems determined by the CIE that can be used for measurement.[27] The $L^*a^*b^*$ system was chosen for this study because it best quantifies colour as perceived by the human eye.[28] The L^*, a^*, and b^* are obtained, using a nonlinear transformation, from the CIE *XYZ* colour space system, where *X*, *Y* and *Z* are the tristimulus values of the perceived colour. L^* is an index of brightness, $+a^*$ is an index of redness and $-a^*$ is an index of greenness, $+b^*$ is an index of yellowness and $-b^*$ is an index of blueness. The equipment measures the difference in the indices ΔL^*, Δa^* and Δb^* between the object and a white standard when both are illuminated with the same standard source. In this case the source was D_{65}, which approximates to average daylight. An object having positive values for these differences would be brighter, more red or less green and more yellow or less blue than the standard.

3. Results

To verify whether the reformulated bodies had resemblance with commercial bone china bodies, the fired samples of commercial and reformulated bone china bodies were analysed by X-ray diffraction technique. Fig. 2 shows the X-ray diffraction traces of a reformulated body (BCM-13) and a commercial bone china body. Commercial bone china bodies contain β-tricalcium phosphate (β-TCP), triclinic anorthite and α-quartz phases labelled as P, A, and Q respectively. As can be seen from Fig. 2, except the formation of minor phase of quartz the reformulated body developed two major crystalline phases namely, β-TCP and anorthite as commercial body. By comparing the intensities of peaks, it would be claimed that the amounts of phases were different. As would be expected the reformulated body developed more anorthite but less β-tricalcium phosphate than commercial body. Similar results were also obtained from the other reformulated body compositions but they are not given here to eliminate the repetition.

The measured thermal expansion coefficient values of reformulated and commercial bone china bodies are given in Table 4. As would be expected the reduction in bone ash content of reformulated bone china bodies has lowered the

Table 4
Thermal expansion coefficient values of reformulated and commercial bone china bodies

	Composition codes						
	BCM-11	BCM-12	BCM-13	BCM-14	BCM-15	BCM-16	Commercial bone china
TEC ($\times 10^{-6}\,^{\circ}C^{-1}$)	7.0	5.4	5.1	6.4	4.9	6.0	8.5

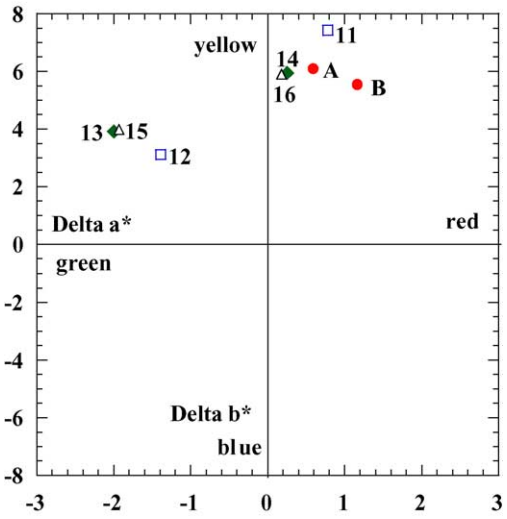

Fig. 3. The colour difference map for reformulated bone china bodies and commercial bone china products A and B.

TEC values significantly. The initial reduction of bone ash content from 50 to 35% reduced the TEC value from 8.5 × $10^{-6}\,^{\circ}C^{-1}$ to 5.4 × $10^{-6}\,^{\circ}C^{-1}$ and further reduction of bone ash content down to 25% level reduced the TEC value to 4.9 × $10^{-6}\,^{\circ}C^{-1}$. This is because of the reduction in the amount of β-TCP crystalline phase, which has relatively higher TEC value. There were also slight differences between the TEC values of pair compositions depending on whether or not containing ZnO.

When the samples of reformulated bodies not containing any ZnO were hold against the daylight a distinctive bluish-green tint was detected. However, the reformulated bodies containing ZnO did not show any discolouration. In order to understand the effect of ZnO addition on colour, the colours of both the reformulated and commercial bone china samples were measured. The CLAB colour difference map for the reformulated bone china samples is given in Fig. 3. On this map the colour difference values for two samples of commercial bone china (A and B) are also plotted. It can be seen that three compositions namely, BCM-11, BCM-14, BCM-16 (11, 14, 16) lie in the upper right quadrant with coordinates, in varying degrees, similar to those for the commercial bone chinas. On the other hand, other compositions namely, BCM-12, BCM-13, BCM-15 (12, 13, 15) lie in the upper left quadrant and they are more green in colour than both the commercial bone chinas and ZnO containing reformulated bone china bodies.

The comparison of colours of the reformulated bone china bodies with each other shows that a significant change in colour resulted from a small change in compositions. That is, all the reformulated bodies which showed similar whiteness with respect to the commercial bone chinas, contained about 5% ZnO. However, all the reformulated bodies, which are more green in colour than commercial bone chinas, did not contain any ZnO.

The addition of ZnO into the body formulation made the difference on the phases that formed in the microstructure. Fig. 4 compares the X-ray traces obtained from BCM-14 and BCM-13, respectively. The X-ray trace for BCM-14 shows the presence of anorthite, β-TCP and zinc-spinel (gahnite, $ZnAl_2O_4$) crystals, however, in the X-ray trace for BCM-13 no gahnite peaks are observed. Figs. 5 and 6 are the SEM images of the microstructures and EDX spectra from the polished and etched specimens of BCM-13 and BCM-14, respectively. Exposure of samples to dilute HF etching solution dissolved the glassy phase, and left the crystals unattacked and this made possible to detect the obvious microstructural difference between these samples. The difference is the detection of gahnite crystals only in the microstructure of BCM-14. Fig. 5 shows the gross microstructure and EDX spectrum of BCM-13, which consists of agglomerates of nodular β-TCP (1–5 μm individual crystallites, labelled as P) and tabular, anorthite grains (1–5 μm, labelled as A). Also the EDX spectrum obtained from the micrograph of BCM-13 detected Ca, P, Al, Si and O indicating β-TCP and anorthite crys-

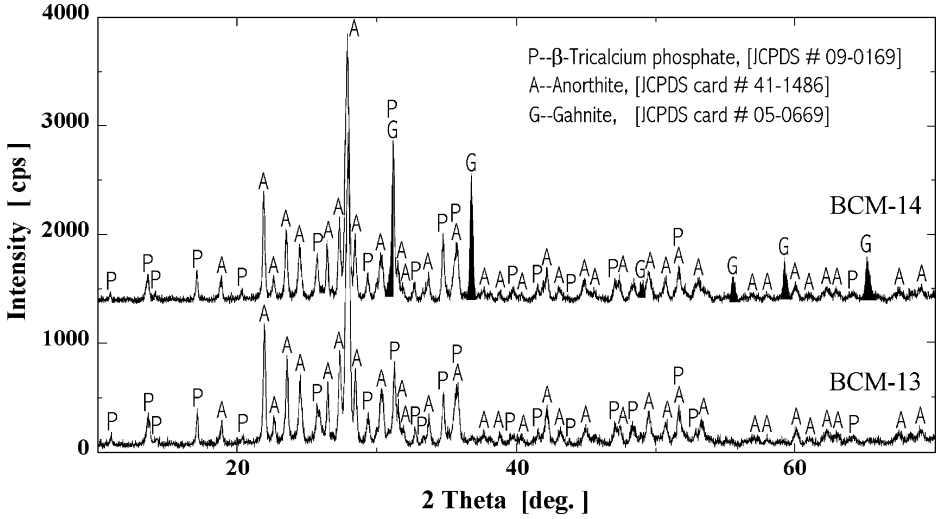

Fig. 4. The effect of ZnO addition on the XRD traces of reformulated bone china bodies.

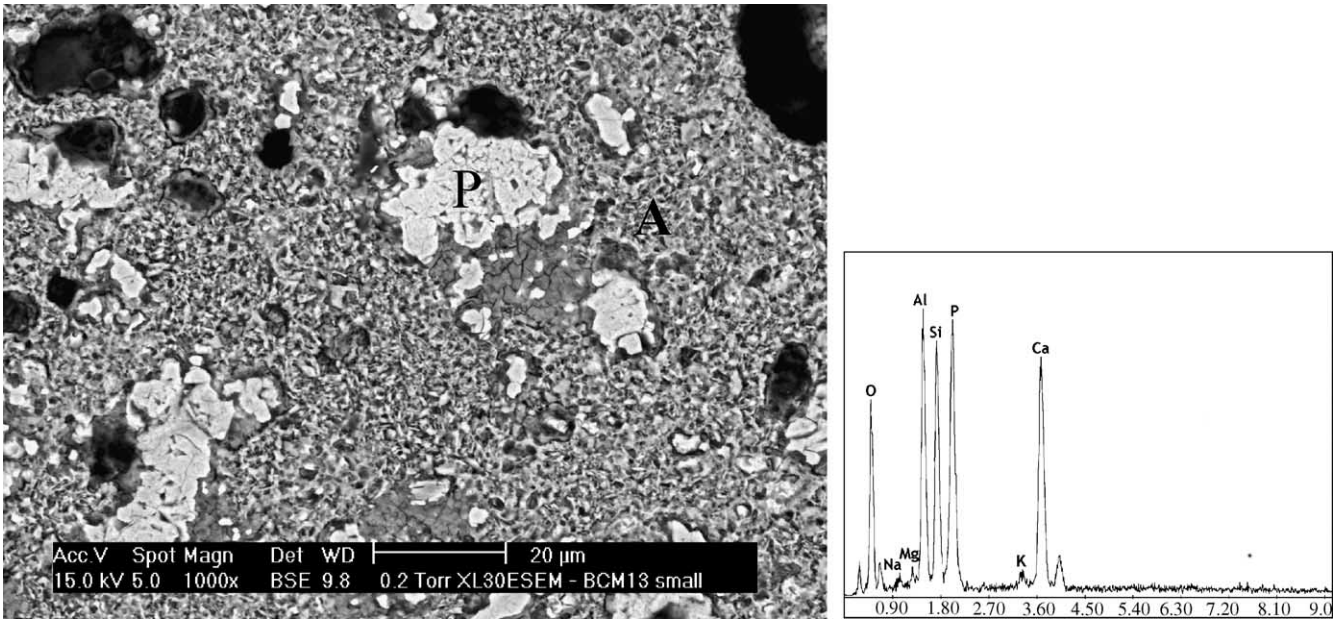

Fig. 5. A typical BSE image and EDX spectrum of the reformulated bone china body not containing any ZnO.

tals formation. As can be seen in Fig. 6a and b the gross microstructure of BCM-14 contains additional faceted, cubic zinc-spinel (gahnite) crystals (0.5–1 μm, labelled as G in Fig. 6b) on top of nodular β-TCP and tabular, anorthite crystals. On the contrary to the EDX spectrum of BCM-13, the detection of additional Zn in the EDX spectrum of BCM-14 (Fig. 6c) also supports the formation of zinc-spinel. These results match well with the XRD results that ZnO containing reformulated bone china bodies develop an additional phase (zinc-spinel crystals) in the microstructure.

According to Wilson[21] discolouration could be caused by wrong firing atmospheres, and it is generally held that a bluish colour results when the kiln atmosphere is reducing. In order to verify this statement the green samples of reformulated bone china bodies, both ZnO containing and the one that does not contain any ZnO, were fired from room temperature to

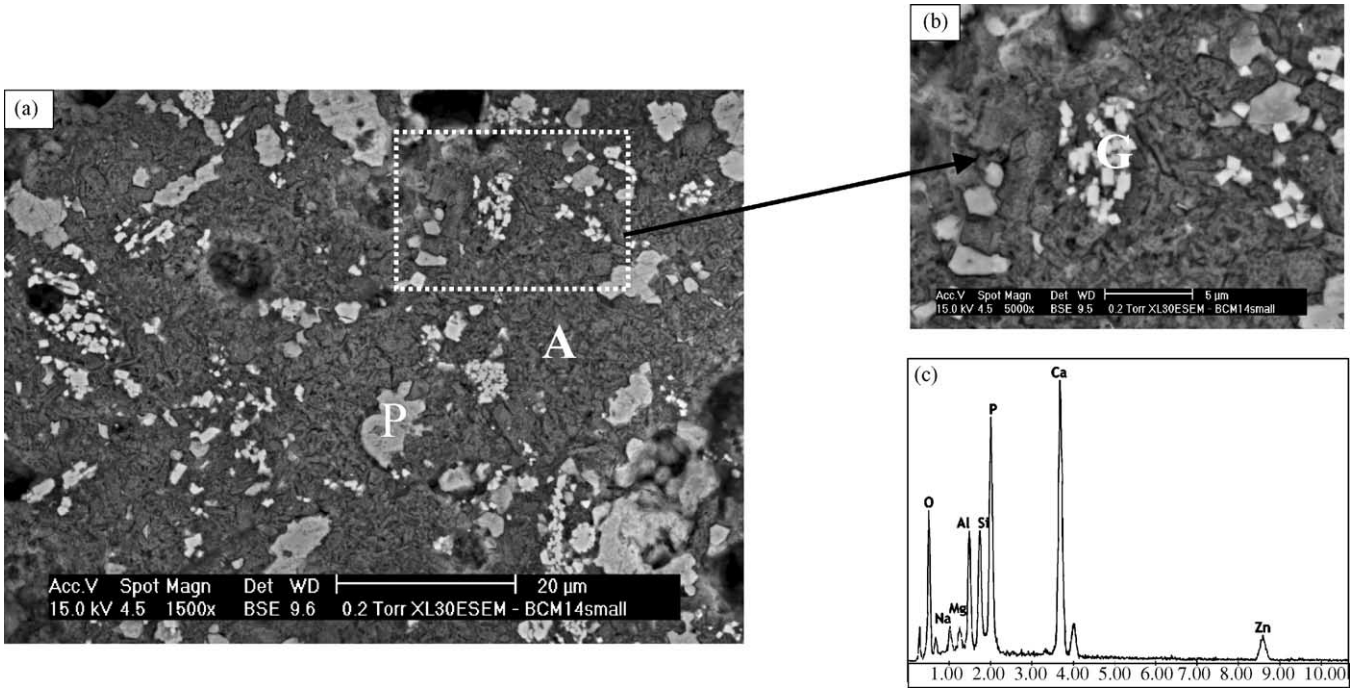

Fig. 6. (a) A typical BSE image of ZnO containing reformulated bone china body. (b) A detailed BSE image of the microstructure shown in (a) indicating the zinc-spinel crystals. (c) A typical EDX spectrum of ZnO containing reformulated bone china body.

the densification temperature in a controlled mild reductive atmosphere by flowing 5% H_2/95% N_2 mixture through the alumina tube at 200 $cm^3\,min^{-1}$. It was found that even in a weakly reducing atmosphere all the fired samples of reformulated bone china bodies turned metallic grey colour rather than producing a bluish-green tint and were totally opaque.

Superior translucency of bone china arises from a good match of refractive indices of the two types of crystals and glassy phases in its microstructure. Since the fired reformulated bone china bodies developed the same crystalline phases as fired commercial bone china, the degree of their translucency would be comparable. Visual examination of the fired reformulated bone china indicated that they exhibited significant degree of translucency. However, the degree of translucency of reformulated bodies containing ZnO was slightly lower than that of reformulated bodies prepared without ZnO. This was because ZnO containing reformulated bodies have an additional crystalline phase (zinc-spinel, gahnite) which has slightly higher refractive index[29] than the other crystalline and glassy phases in the microstructure. The measurement of translucency is difficult and was considered to be outside the scope of this study. The only significant difference between the reformulated bone china, and commercial bone china, was the former's bluish-green tint which has been eliminated by the addition of ZnO.

4. Discussion

The microstructure of a modern bone china contains discrete regions of agglomerated, spheroidal β-TCP and lath-like anorthite crystals in calcium aluminosilicate glass along with a small proportion (∼3 vol.%) of angular α-quartz grains.[12–14] The microstructure of a reformulated bone china body (the one that does not contain any ZnO) also, except α-quartz grains, contains the same phases with different proportions. However, although the modern bone china has a creamy-white colour, the reformulated bone china has a bluish-green tint. It is anticipated that the reason for colouring is the iron impurity, which comes from raw materials in the form of oxide (Fe_2O_3). This impurity can take on various valence states (Fe^{2+}, Fe^{3+}) depending on their concentrations, and the temperature and oxygen pressure of the firing atmosphere. The most possible impurities, which could be in the bone china bodies, were Mg, K, Na and Fe.[8] Among these Na and K are the glass forming elements. The colouring effect of iron in glassy phase is greenish-blue.[22] It would be expected that iron impurity in glassy phase of modern bone china and reformulated one would make the both ceramic body to show greenish-blue colour, in fact the modern bone china is creamy-white. This is explained by Parmelee[30] as follows: The P_2O_5 in glass phase has a bleaching effect on colour. The same bleaching effect has not been observed in reformulated bone china not containing ZnO, since the amount of P_2O_5 in reformulated bone china was relatively very low. For the colouring mechanism of Fe in glass, one could refer to Weyl.[31] Briefly, simultaneous presence of iron ions Fe^{2+} and Fe^{3+}, in the same molecules would lead to a greenish-blue colour.

The following is an attempt to explain the elimination of colouring by ZnO addition to the reformulated bone china. It has been shown experimentally, that the introduction of ZnO into the body develops zinc-spinel (gahnite) crystals, which is capable of incorporating both the divalent (Fe^{2+}) and trivalent (Fe^{3+}) iron in its structure[29,32] and hence take the irons ions out of glassy phase. Zinc aluminate has a spinel structure, which is an approximately close packed face-centered cubic array of anions with holes partly filled by the cations. A wide variety of ion sizes and charges, including Fe^{3+} and Fe^{2+}, can fit into the spinel structure.[29] In particular; Fe^{3+} ions are mainly incorporated into the (AlO_6) octahedra, substituting for Al^{3+}. Takashima[33] studied the behaviour of Cr^{3+} and Fe^{3+} ions in the gahnite crystallized from zinc opaque glazes and showed that almost all the Fe^{3+} ions migrated into the gahnite (zinc-spinel) phase. Djemai et al.[34] postulated that the increased whiteness of mullite samples, which contain iron oxide impurities, by iron incorporation into mullite structure.

Similarly, in this study a relationship was established between the increased whiteness of the reformulated bone china bodies and zinc-spinel formation, which is thought to be incorporating the iron inclusions into its structure and eliminating the formation of a chromophore group, Fe^{3+}–O–Fe^{2+}.

5. Conclusions

1. The reduction of bone ash content of bone china from 50 to 25 wt.% reduced the TEC from $8.5 \times 10^{-6}\,°C^{-1}$ to $4.9 \times 10^{-6}\,°C^{-1}$ which could match certain high scratch resistance glazes.
2. Reformulated bone china showed a bluish green tint due to reduction of bone ash content. Addition of about 5 wt.% of ZnO to the reformulated body completely eliminated the bluish-green tint. The formation of zinc-spinel crystals is responsible for the increasing whiteness by incorporating iron ions.

References

1. Messer, P. F., Hand, R. J., West, S., Batista, S., Capoglu, A., Kiang, M. K. *et al.*, Design and development of a low-clay translucent tableware for severe service conditions. *Br Ceram Proc*, 1999, **60**(2), 347–348.
2. Cubbon, R. C. P., Consumer and environmental pressure on the use of lead glazes and colours. *Interceramic*, 1994, **43**(4), 240–242.
3. Alsop, S., Development of unleaded glazes for ceramic tableware. *Br Ceram Trans*, 1994, **93**(2), 77–79.
4. Jackson, P. R., Unleaded glazes and colours for tableware-an update. *Br Ceram Trans*, 1995, **94**(4), 171–173.
5. Kara, A. and Stevens, R., Interactions between an ABS type leadless glaze and a biscuit fired bone china body during glost firing. Part I: preparation of experimental phases. *J Eur Ceram Soc*, 2002, **22**(7), 1095–1102.

6. Kara, A. and Stevens, R., Interactions between an ABS type leadless glaze and a biscuit fired bone china body during glost firing. Part II: investigation of interactions. *J Eur Ceram Soc*, 2002, **22**(7), 1103–1112.
7. Kara, A. and Stevens, R., Interactions between an ABS type leadless glaze and a biscuit fired bone china body during glost firing. Part III: effect of glassy matrix phase. *J Eur Ceram Soc*, 2003, **23**(10), 1617–1628.
8. Rado, P., Bone china. *Ceramic Monographs—Handbook of Ceramics*. Verlag Schmid GmbH Freiburg i. Brg, 1981.
9. Dinsdale, A., *Pottery Science Materials, Process & Products*. John Wiley & Sons, Chichester, UK, 1986.
10. Pierre, P. D., Constitution of bone china: I. High temperature phase equilibrium studies in the system tricalcium phosphate-anorthite-silica. *J Am Ceram Soc*, 1954, **37**(6), 243–258.
11. Taylor, D., A study of some of the changes in bone china and whiteware during firing. *Trans J Br Ceram Soc*, 1979, **78**, 43–74.
12. Iqbal, Y., Messer, P. F. and Lee, W. E., The non-equilibrium microstructure of bone china. *Br Ceram Trans*, 2000, **99**(3), 110–116.
13. Kara, A. and Stevens, R., Characterisation of biscuit fired bone china body microstructure. Part I: XRD and SEM of crystalline phases. *J Eur Ceram Soc*, 2002, **22**(5), 731–736.
14. Kara, A. and Stevens, R., Characterisation of biscuit fired bone china body microstructure. Part II: transmission electron microscopy (TEM) of glassy matrix. *J Eur Ceram Soc*, 2002, **22**(5), 737–743.
15. Ryu, B. and Yasui, I., Sintering and crystallization behaviour of a glass powder and block with a composition of anorthite and the microstructure dependence of its thermal expansion. *J Mater Sci*, 1994, **29**, 3323–3328.
16. Oldfield, L. F., Absolute and relative linear thermal expansion coefficients of vitreous silica and platinum. *Glass Technol*, 1964, **5**(1), 41–50.
17. Gratton, D., Replacing bone ash in China. *J Can Ceram Q*, 1996, **4**, 242.
18. Yates, W. H. and Ellam, H., A study of the bone china body. Part I: colour. *Trans Ceram Soc*, 1917–1918, **17**, 120.
19. Mellor, Recent research on the bone china body. *Trans Ceram Soc*, 1918–1919, **18**, 497–509 (abstracted in *J Am Ceram Soc*, 1920, **3**(5), 429).
20. Moore, Cause and prevention of brown colouration in china bodies in the Enamel Kiln. *Trans Ceram (England)*, 1905–1906, **5**, 37–44.
21. Wilson, S. T., Atmosphere for China biscuit ovens. *Trans Engl Ceram Soc*, 1909–1910, **9**, 17.
22. Rawson, H., *Properties and Applications of Glass*. *Glass Science and Technology*, *Vol 3*. Elsevier, 1980.
23. Herring, A. P., Dean, R. W. and Drobnick, J. L., *Glass Ind*, 1970, **51**, 316–322, 350–356, 394–399.
24. Capoglu, A. and Messer, P. F., Design and development of a chamotte for use in a low-clay translucent whiteware. *J Eur Ceram Soc*, 2004, **24**(7), 2067–2072.
25. Jarcho, M., Bolen, C. H., Thomas, M. B., Bobick, J., Kay, J. F. and Doremus, R. H., Hydroxylapatite synthesis and characterisation in dense polycrystalline form. *J Mater Sci*, 1976, **11**, 2027–2035.
26. Billmeyer Jr., F. W. and Saltzman, M., *Principles of Color Technology*. Wiley, 1966.
27. MacAdam, D. L., *Optical Sciences, Color Measurement*. Springer-Verlag, Berlin, Heidelberg, New York, 1981.
28. Berger-Schunn, A., *Practical Color Measurement: A Primer for the Beginner, a Reminder for the Expert*. Wiley, 1994.
29. Richerson, D. W., *Modern Ceramic Engineering: Properties, Processing, and Use in Design*. Marcel Dekker, Inc., New York, 1992.
30. Parmelee, C. W., The action of phosphoric acid in body mixtures. *Trans Am Ceram Soc*, 1908, **8**, 236.
31. Weyl, W. A., *Coloured Glasses*. Society of Glass Technology, Sheffield, England, 1978.
32. Chiang, Y.-T., Birnie, D. and Kingery, W. D., *Physical Ceramics: Principles for Ceramic Science and Engineering*. John Wiley & Sons, New York, 1997.
33. Takashima, H., Behaviour of Cr^{3+} and Fe^{3+} ions in the gahnite crystallized from zinc opaque glazes. *Ceram Int*, 1982, **8**(2), 74–76.
34. Djemai, A., Calas, G. and Muller, J. P., Role of structural Fe(III) and oxide nanophases in mullite coloration. *J Am Ceram Soc*, 2001, **84**(7), 1627–1631.